



Theoretical Bio-significance Evaluation of Quinazoline Analogues

Oyebamiji, Abel Kolawole^{1,2} and Adeleke, Babatunde Benjamin^{3*}

¹Department of Pure and Applied Chemistry, Ladoke Akintola University of Technology, P.M.B. 4000, Ogbomoso, Oyo State, Nigeria.

²Department of Basis Science, Faculty of Sciences, Adeleke University, P.M.B. 250, Ede, Osun State, Nigeria.

³Department of Chemistry, University of Ibadan, Ibadan, Nigeria.

Authors' contributions

This work was carried out in collaboration between both authors. Both authors read and approved the final manuscript.

Article Information

DOI: 10.9734/IRJPAC/2019/46543

Editor(s):

(1) Dr. Bengi Uslu, Department of Analytical Chemistry, Ankara University, Ankara-Turkey.

Reviewers:

(1) Ruswanto, STIKes Bakti Tunas Husada Tasikmalaya, Indonesia.

(2) Sarbani Pal, MNR Degree and PG College, India.

(3) Manojit Pal, Dr Reddy's Institute of Life Sciences, Hyderabad, India.

Complete Peer review History: <http://www.sdiarticle3.com/review-history/46543>

Original Research Article

Received 08 November 2018

Accepted 24 January 2019

Published 13 February 2019

ABSTRACT

Structure of nine quinazoline derivatives were optimized using density functional theory method in order to probe into the bioactive conformations of the compound. The obtained descriptors which described the anti-neuroepithelioma activity of the compounds were selected and used to develop a model using partial least square method. The developed model replicated the experimental IC₅₀ indicative of the predicting power of the model. In addition, ligand-receptor interactions are reported and 2-((E)-2-(4-Bromo-phenyl)-vinyl)-3H-quinazolin-4-one (A₄) showed the greatest affinity to bind on the active site of human neuroepithelioma cell line.

Keywords: QSAR; DFT; quinazoline analogues; docking; neuroepithelioma cell line.

*Corresponding author: E-mail: adelekebb46@gmail.com, abeloyebamiji@gmail.com;

1. INTRODUCTION

Several natural and synthetic quinazoline based products as antimicrobial agents have been successfully developed over the last four decades [1,2]. Quinazoline, a heterocyclic compound with molecular formula, $C_8H_6N_2$, has a double-ring structure consisting of a benzene ring fused with pyrimidine ring, and exists as yellow crystals [3,4]. Quinazoline and its derivatives have shown various biological activities as antidepressant, anti-inflammatory, antimalarial, anticancer, antifungal, antimicrobial, antiviral, anti-tubercular, anti-protozoan, anticonvulsant [5-8].

Quantitative Structural Activity Relationship (QSAR) is a numerical model that link series of molecular parameters of a molecules to its bioactivity [9]. In the discovery, design and development of drug-like molecules, quantitative structural activity relationship has gained a vast usefulness which has drawn several researchers to studying bioactivity of compounds via QSAR [10].

The use of docking as a means of studying the connectivity that is existing between ligands and enzyme (receptor) has been extensively recognized. It shows the basic ways that drug-like compounds used in preventing targeted binding site [11,12].

Bio-significance of molecular compounds is determined by the structure and the electronic properties of the molecules. Thus, in this work, the optimised structure and electronic properties of 2-((E)-Styryl)-3H-quinazolin-4-one (A_1), 2-((E)-2-(2-Methoxy-phenyl)-vinyl)-3H-quinazolin-4-one (A_2), 2-((E)-2-(3-Methoxy-phenyl)-vinyl)-3H-quinazolin-4-one (A_3), 2-((E)-2-(4-Bromo-phenyl)-vinyl)-3H-quinazolin-4-one (A_4), 4-Chloro-2-((E)-styryl)-quinazoline (B_1), 4-Chloro-2-((E)-2-(2-

methoxy-phenyl)-vinyl)-quinazoline (B_2), 4-Chloro-2-((E)-2-(3-methoxy-phenyl)-vinyl)-quinazoline (B_3), 4-Chloro-2-((E)-2-(4-methoxy-phenyl)-vinyl)-quinazoline (B_4) and 4-Chloro-2-((E)-2-(2,4-dimethoxy-phenyl)-vinyl)-quinazoline (B_5) were computed using quantum chemical method with a view to theoretically investigate the anti-human neuroepithelioma activity of the compounds through the development of a quantitative structural activity relationship, QSAR and molecular docking study. This set of nine quinazoline derivatives have been experimentally shown to have expressive bioactivity against human neuroepithelioma [13].

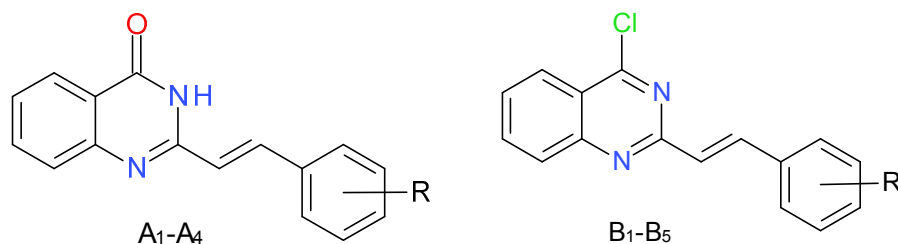
2. MATERIALS AND METHODS

2.1 Optimization

The studied compounds (Fig. 1) were optimized using density functional theory via 6-31G* basis set. The density functional theory method used in this work was done with B3LYP density functionals which include Becke's gradient exchange [14] and Lee, Yang and Parr correlation [15]. The accuracy of density functional theory calculations is based on the selected basis set. Among the calculated descriptors are the highest occupied molecular orbital (E_{HOMO}) energy, lowest unoccupied molecular orbital (E_{LUMO}) energy, dipole moment, chemical potential, chemical hardness, etc. The quantum chemical calculations were done using Spartan '14 software by wavefunction Inc [16].

2.2 Descriptor Selection and QSAR Model Development

The study of quantitative structure activity relationship (QSAR) require the use of appropriate molecular descriptors (with high simplicity and high predicting power) from the



A_1 : H, A_2 : 2-OMe, A_3 : 3-OMe, A_4 : 4-Br, B_1 : H, B_2 : 2-OMe, B_3 : 3-OMe, B_4 : 4-OMe, B_5 : 2, 4-OMe.

Fig. 1. Schematic structures of the studied Quinazolines

entire calculated descriptors [17,18]. Therefore, QSAR model was developed via partial least square method and this was used to calculate the predicted bioactivity. The software used for partial least square method was XLSTAT 2018 [19].

2.3 Quality and Validation of QSAR Model

The evaluation of the quality and validation of developed QSAR model were done by considering cross validation ($C_v.R^2$) and adjusted R^2 (R_{adj}^2) [Equation 1 and 2].

$$C_v.R^2 = 1 - \frac{\sum(Y_{obs}-Y_{cal})^2}{\sum(Y_{obs}-\bar{Y}_{obs})^2} \quad (1)$$

The adjusted R^2 could be calculated using equation (2)

$$R_a^2 = \frac{(N-1) \times R^2 - P}{N-1-P} \quad (2)$$

The developed quantitative structural activity relationship model could be considered prognostic, if $C_v.R^2 > 0.5$ and $R_{adj}^2 > 0.6$ [20-22].

2.4 Molecular Docking Studies

Molecular docking studies were performed by using the following softwares; Discovery Studio 4.1, Autodock tools 1.5.6, Autodock vina 1.1.2, and pymol 1.7.4.4. The receptor used in this work was obtained from protein data bank and adjusted for docking purpose. For the purpose of accuracy in docking, the residues (water molecules and crystallized drug-like molecules) were removed from the protein (4bjx) [23]. The treated receptor was subjected to autodock tool 1.5.6 for location of binding site and development of a grid box (centre grid box: x:-3.872; y:-4.818; z:-18.982) to cover the neuroepithelioma cell line binding site. Autodock vina software was employed to simulate the ligand into the active site of the receptor (protein) in order to calculate the binding energy of the ligand-receptor complexes. Also, inhibition constant was calculated using equation 3.

$$K_i = e^{\frac{-\Delta G}{RT}} \quad (3)$$

3. RESULTS AND DISCUSSION

3.1 Electronic Descriptors and QSAR Studies

The calculated descriptors include E_{HOMO} , E_{LUMO} , dipole moment (DM), Log P, molecular weight

(MW), polar surface area (PSA), polarizability and ovality (Table 1).

The calculated descriptors were used as independent variables and the experimental IC_{50} (Table 2), served as dependent variables in the development of QSAR model using multiple linear regression. This was used to select the molecular parameters that perfectly describe anticancer activity of quinazolines. The developed QSAR model (Equation 4) was used to predict the bioactivity of the studied compounds (Table 2). The calculated squared correlation coefficient (R^2) (0.947) and the adjusted R^2 (0.894) revealed the predicting power and quality of the model developed as shown in Table 3. The model reproduced the observed IC_{50} as depicted by the residual values (Observed IC_{50} – Predicted IC_{50}) (Table 2).

$$IC_{50} = -597.570 - 10.5191(\text{LOGP}) + 21.8795(\text{HET}) - 59.9882(\text{LUMO}) - 891.799(\text{N1}) \quad (4)$$

This developed QSAR model as shown in equation 4 shows a positive input of Heteroatom. However, log P, LUMO and Charge on Nitrogen (1) (N1) contributed negatively to the bioactivity and this was suggesting that, as log P, LUMO and Charge on Nitrogen (1) (N1) decreases, biological activity of Quinazoline derivatives increases and vice-versa for Heteroatom. The QSAR model showed that the anticancer activity of the compounds was directly linked to these molecular parameters. Fig. 2 demonstrates the quality of the developed QSAR while as shown in Fig. 3, the residual values were observed on both positive and negative sides of the graph and this indicated that there was no systemic inaccuracy in the developed QSAR model.

4. DOCKING STUDIES

The study of molecular docking was executed in this research in order to comprehend the binding mode of drug-like molecule against the receptor (4bjx). First and foremost, Ramachandran plot was used to evaluate the orientation and conformation of human neuroepithelioma cell line (PDB ID: 4bjx), and it was discovered that almost all the residue in the studied receptor (i.e. 99.2% of the residues) was found in a favoured region and the entire residues (i.e. 100.0% of the residues) were in allowed regions. More so, there were no outliers as shown in Fig. 4. Thus, the receptor used in this work was stable and of a good quality. As shown in Table 4, the dock

Table 1. The calculated molecular descriptors obtained for quinazoline derivatives

Comp	HOMO (eV)	LUMO (eV)	BG (eV)	DM (Debye)	LOGP	MW	OVALITY	PSA (Å ²)	HBD	HBA	POL	IC ₅₀
A ₁	-6.04	-1.70	4.34	4.12	3.39	248.285	1.40	32.085	0	2	61.55	1.39
A ₂	-6.02	-1.74	4.28	4.82	3.26	278.311	1.42	39.584	0	4	63.56	2.88
A ₃	-5.98	-1.73	4.25	5.71	3.26	278.311	1.46	39.100	0	3	63.77	5.13
A ₄	-6.05	-1.80	4.25	2.16	4.22	327.181	1.44	32.079	0	2	63.04	2.85
B ₁	-6.16	-2.28	3.88	3.10	4.83	266.731	1.41	13.636	0	3	62.18	4.96
B ₂	-5.91	-2.37	3.54	4.05	4.71	297.757	1.46	20.169	0	3	64.41	0.58
B ₃	-5.96	-2.41	3.55	3.72	4.71	296.757	1.46	20.935	0	8	64.40	5.28
B ₄	-5.78	-2.37	3.41	4.35	4.71	296.757	1.46	20.938	0	2	64.43	4.34
B ₅	-5.72	-2.35	3.37	2.93	4.58	326.783	1.51	26.775	0	3	66.64	1.75

scores for ligand-receptor complexes ranged from -8.2 to -7.6 kcal/mol and it was discovered that A₄ had the highest possibility to inhibit human neuroepithelioma cell. The residues involve in the interaction between studied compounds (A₁-B₅) and 4bjx were VAL-87, CYS-136, LEU-92, TRP-81, PRO-82 for A₁, LEU-92, TRP-81, VAL-87, ASN-140, PRO-82, CYS-136, ILE-146 for A₂, ASN140, CYS-136, PRO82, GLN-85, LEU-92, LYS-91, ILE-146, VAL-87 for A₃, ASN140 and PRO82 for A₄, CYS-136, VAL-

87, LEU-92, PRO-82, ILE-146, TRP-81 for B₁, VAL-87, CYS-136, LEU-92, PRO-82, TRP-81 for B₂, MET-132, MET-105, PRO-82, TRP-81, VAL-87, ILE-146, CYS-136, LEU-92 for B₃, LEU-92, VAL-87, CYS-136, ILE-146, MET-105, TRP-81 for B₄ and CYS-136, ILE-146, VAL-87, GLN-85, LEU-92, TRP-81, TYR-97, LEU-94, TYR-139 for B₅. The ligand and receptor complex displayed in Figure 5 showing the residue that was involved in the interaction together with hydrogen bonds for A₄.

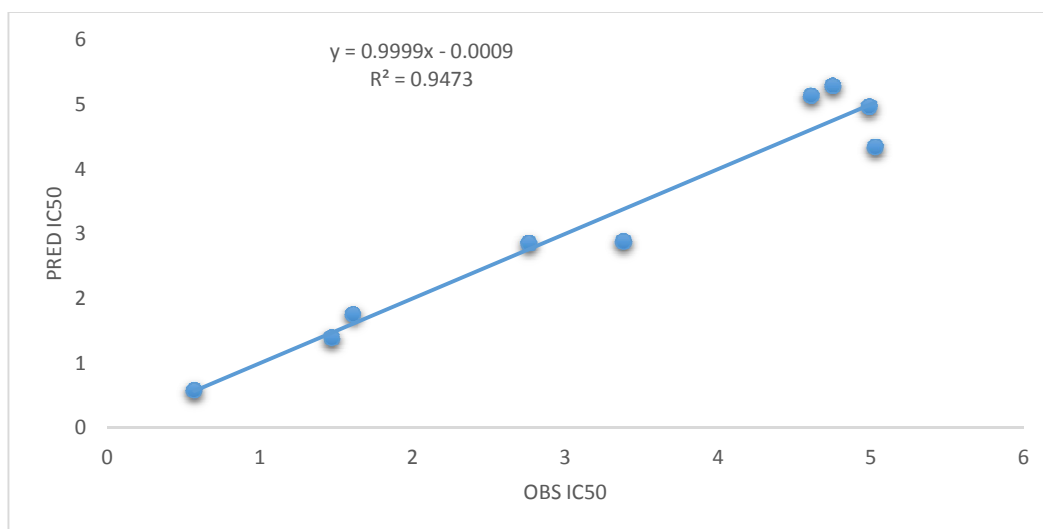


Fig. 2. Plot of predicted IC₅₀ against observed IC₅₀

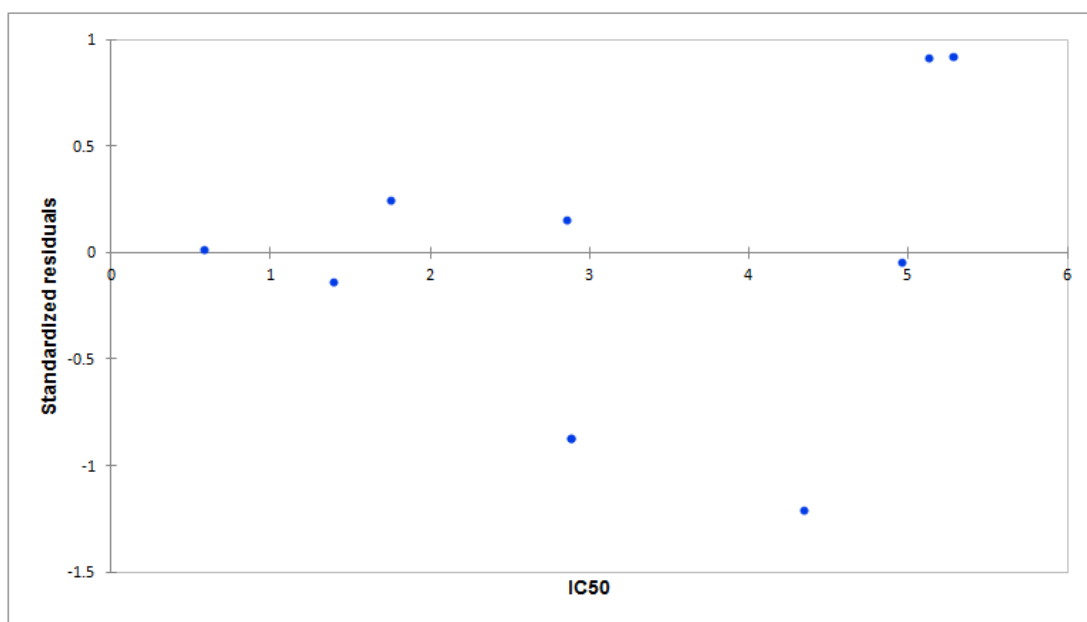


Fig. 3. Plot of residual values against observed IC₅₀

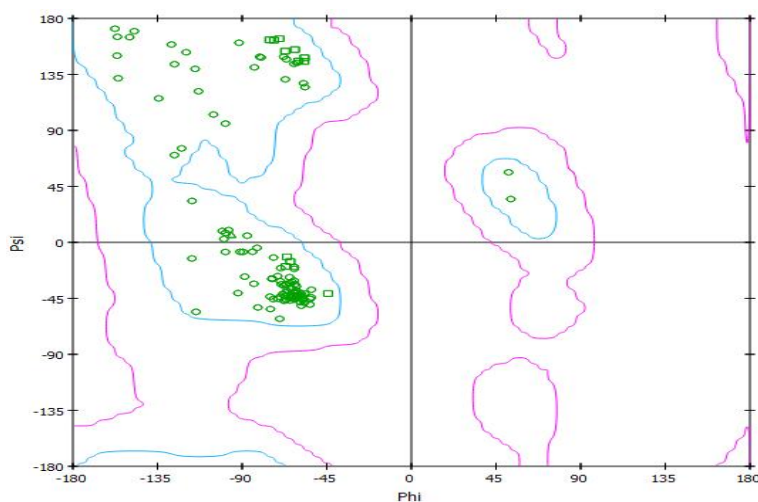


Fig. 4. Ramachandran plot for human neuroepithelioma cell line (PDB ID: 4bjx) [23]

Table 2. Observed IC₅₀ and predicted IC₅₀

	Observed IC ₅₀	Predicted IC ₅₀	Residual
A ₁	1.39	1.47	-0.08
A ₂	2.88	3.38	-0.50
A ₃	5.13	4.61	0.52
A ₄	2.85	2.76	0.09
B ₅	4.96	4.99	-0.03
B ₆	0.58	0.57	0.01
B ₇	5.28	4.75	0.53
B ₈	4.34	5.03	-0.69
B ₉	1.75	1.61	0.14

Table 3. Statistical parameters for developed QSAR model

N	p	R ²	R ² _{adj}	CV.R ²
9	4	0.947	0.894	0.984

Table 4. Ligand-receptor dock score of quinazoline derivatives with 4bjx

Compound	Affinity (kcal/mol)	K _i (μM)	Interacting Residues
A ₁	-8.1	8.72 x 10 ⁵	VAL-87, CYS-136, LEU-92, TRP-81, PRO-82
A ₂	-8.0	7.37 x 10 ⁵	LEU-92, TRP-81, VAL-87, ASN-140, PRO-82, CYS-136, ILE-146
A ₃	-8.1	8.72 x 10 ⁵	ASN140, CYS-136, PRO82, GLN-85, LEU-92, LYS-91, ILE-146, VAL-87
A ₄	-8.2	1.03 x 10 ⁶	ASN140 and PRO82
B ₁	-8.1	8.72 x 10 ⁵	CYS-136, VAL-87, LEU-92, PRO-82, ILE-146, TRP-81
B ₂	-8.1	8.72 x 10 ⁵	VAL-87, CYS-136, LEU-92, PRO-82, TRP-81
B ₃	-7.8	5.25 x 10 ⁵	MET-132, MET-105, PRO-82, TRP-81, VAL-87, ILE-146, CYS-136, LEU-92
B ₄	-7.7	4.44 x 10 ⁵	LEU-92, VAL-87, CYS-136, ILE-146, MET-105, TRP-81
B ₅	-7.6	3.75 x 10 ⁵	CYS-136, ILE-146, VAL-87, GLN-85, LEU-92, TRP-81, TYR-97, LEU-94, TYR-139

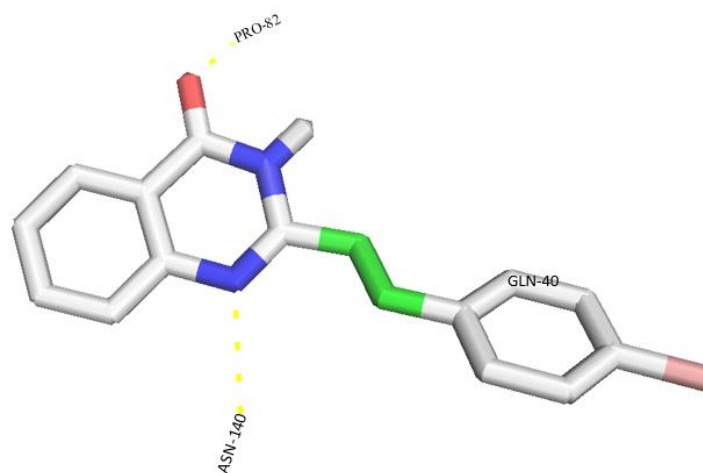


Fig. 5. Interactions of A_4 with the residue in the active gouge of human neuroepithelioma cell line (4bjx)

Also, Lipinski's rule of five was observed for the compounds used in this work and all the studied compounds proved to be drug-like compounds. As shown in Table 1, the molecular weight value were ≤ 500 , Hydrogen bond acceptor were ≤ 10 , Hydrogen bond donor were less than ≤ 5 and calculated logP value were also ≤ 5 .

5. CONCLUSION

The anti-human neuroepithelioma activity of quinazoline analogues was observed using theoretical approach. In this study, density functional theory was use to optimized the molecular compounds and the descriptors obtained were used for QSAR analysis using partial least square method. The descriptors, E_{HOMO} , E_{LUMO} , Log P, ovality, PSA, and molecular weight were implicated in the anti-human neuroepithelioma activity of quinazoline derivatives and the developed QSAR model replicated the experimental IC_{50} . Also, 2-((E)-2-(4-Bromo-phenyl)-vinyl)-3H-quinazolin-4-one (A_4) inhibited the 4bjx most as revealed by the affinity and the inhibition constant (K_i).

COMPETING INTERESTS

Authors have declared that no competing interests exist.

REFERENCES

1. Carlos MMG, Vladimir VK. Recent developments on antimicrobial quinoline chemistry, microbial pathogens and strategies for combating them. Science, Technology and Education (A. Méndez-Vilas, Ed.); 2013.
2. Majumdar KC, Chattopadhyay SK. Heterocycles in natural product synthesis. Wiley-VCH, 1-658; 2011.
3. Connolly DJ, Cusack D, O'Sullivan TP, Guiry PJ. Synthesis of quinazolinones and quinazolines. Tetrahedron. 2005;61(43):10153–10202.
4. Abida PN, Arpanarana M. An updated review: Newer quinazoline derivatives under clinical trial. International Journal of Pharmaceutical & Biological Archive. 2011;2(6):1651–1657.
5. El-Messery SM, Hassan GS, Al-Omary FAM, El-Subbagh HI. Substituted thiazoles VI. Synthesis and antitumor activity of new 2-acetamido- and 2 or 3-propanamido-thiazole analogues. Eur. J. Med. Chem. 2012;54:615–625.
6. Berest GG, Voskoboynik OY, Kovalenko SI, et al. Synthesis and biological activity of novel N-cycloalkyl-(cycloalkylaryl)-2-[(3-R-2-oxo-2H-[1, 2, 4] triazino [2, 3-c] quinazoline-6-yl) thio] acetamides. Eur. J. Med. Chem. 2011;46:6066–6074.
7. Hu J, Zhang Y, Dong L, et al. Design, synthesis, and biological evaluation of novel quinazoline derivatives as anti-inflammatory agents against lipopolysaccharide-induced acute lung injury in rats. Chem. Biol. Drug Des. 2015;85:672–684.
8. Ammerdorffer A, Stojanov M, Greub G, et al. Chlamydia trachomatis and chlamydia-like bacteria: New enemies of human

- pregnancies. *Curr. Opin. Infect. Dis.* 2017;30:289–296.
9. Hansch C. A quantitative approach to biochemical structure-activity relationships. *Acc of Chem Res.* 1969;2:232-239.
10. Ramsden CA. Quantitative Drug design of comprehensive medicinal chemistry. Oxford. 1990;4.
11. Cherfils J, Janin J. Protein docking algorithms: Simulating molecular recognition. *Curr. Opin. Struct. Biol.* 1993;3:265-269.
12. Kuntz ID, Meng EC, Shoichet BK. Structure-based molecular design. *Acc. Chem. Res.* 1994;27:117-123.
13. Anna MW, Danuta SK, Robert M, Jacek F, Agnieszka S, Katarzyna S, Knas M, Sishir KK, Zaklina K, Josef J, Alicja R, Joanna RW. Investigating the anti-proliferative activity of styrylzanaphthalenes and azanaphthalenediones. *Bioorganic & Medicinal Chem.* 2010;18:2664–2671.
14. Becke AD. Density-functional thermochemistry. III. The role of exact exchange. *J. Chem. Phys.* 1993;98:5648-5652.
15. Lee C, Yang W, Parr RG. Development of the Colle-Salvetti correlation-energy formula into a functional of the electron density. *Condens. Matter. Phys Rev B.* 1988;37(2):785-9.
DOI: 10.1103/PhysRevB.37.785
16. Spartan 14, Wave function, INC, Irvine CA 92612, USA.
17. Learidi R, Boggia R, Terrile M. Genetic algorithms as a strategy for feature selection. *J Chemomet.* 1992;6:267–281.
18. Pourbasheer E, Riahi S, Ganjali MR, Norouzi P. Application of genetic algorithm support vector machine, (GA–SVM) for prediction of BK-channels activity. *Eur. J of Med Chem.* 2009;44:5023–5028.
19. Available:www.xlstat.com
20. Golbraikh A, Tropsha A. Beware of q²! *J Mol Graph Model.* 2002;20:269–276.
21. Marrero PY, Castillo GJA, Torrens F, Romero ZV, Castro EA. Atom, atom-type, and total linear indices of the molecular pseudograph's atom adjacency matrix: Application to QSPR/QSAR studies of organic compounds. *Molecules.* 2004;9(12):1100–1123.
22. Oyebamiji AK, Semire B. DFT-QSAR and docking studies of 2-[5-(aryloxymethyl)-1,3,4-oxadiazol-2-ylsulfanyl] acetic acids derivatives against *Bacillus subtilis*. *Der Pharma Chemica.* 2018;10(3):135-139.
23. Wyce A, Ganji G, Smitheman KN, Chung CW, Korenchuk S, et al. BET inhibition silences expression of *MYCN* and *BCL2* and induces cytotoxicity in neuroblastoma tumor models. *PLoS ONE.* 2013;8(8):e72967.
DOI: 10.1371/journal.pone.0072967

© 2019 Kolawole and Benjamin; This is an Open Access article distributed under the terms of the Creative Commons Attribution License (<http://creativecommons.org/licenses/by/4.0>), which permits unrestricted use, distribution, and reproduction in any medium, provided the original work is properly cited.

Peer-review history:

The peer review history for this paper can be accessed here:
<http://www.sdiarticle3.com/review-history/46543>